



Regulator of G Protein Signaling 2 (RGS2) and RGS4 Form Distinct G Protein-Dependent Complexes with Protease Activated-Receptor 1 (PAR1) in Live Cells

Sungho Ghil¹, Kelly L. McCoy², John R. Hepler^{2*}

¹ Department of Life Science, Kyonggi University, Suwon, Republic of Korea, ² Department of Pharmacology, Rollins Research center, Emory University School of Medicine, Atlanta, Georgia, United States of America

Abstract

Protease-activated receptor 1 (PAR1) is a G-protein coupled receptor (GPCR) that is activated by natural proteases to regulate many physiological actions. We previously reported that PAR1 couples to G_i , G_q and G_{12} to activate linked signaling pathways. Regulators of G protein signaling (RGS) proteins serve as GTPase activating proteins to inhibit GPCR/G protein signaling. Some RGS proteins interact directly with certain GPCRs to modulate their signals, though cellular mechanisms dictating selective RGS/GPCR coupling are poorly understood. Here, using bioluminescence resonance energy transfer (BRET), we tested whether RGS2 and RGS4 bind to PAR1 in live COS-7 cells to regulate PAR1/ $G\alpha$ -mediated signaling. We report that PAR1 selectively interacts with either RGS2 or RGS4 in a G protein-dependent manner. Very little BRET activity is observed between PAR1-Venus (PAR1-Ven) and either RGS2-Luciferase (RGS2-Luc) or RGS4-Luc in the absence of $G\alpha$. However, in the presence of specific $G\alpha$ subunits, BRET activity was markedly enhanced between PAR1-RGS2 by $G\alpha_{q/11}$, and PAR1-RGS4 by $G\alpha_o$, but not by other $G\alpha$ subunits. $G\alpha_{q/11}$ -YFP/RGS2-Luc BRET activity is promoted by PAR1 and is markedly enhanced by agonist (TFLLR) stimulation. However, PAR1-Ven/RGS-Luc BRET activity was blocked by a PAR1 mutant (R205A) that eliminates PAR1- $G_{q/11}$ coupling. The purified intracellular third loop of PAR1 binds directly to purified His-RGS2 or His-RGS4. In cells, RGS2 and RGS4 inhibited PAR1/ $G\alpha$ -mediated calcium and MAPK/ERK signaling, respectively, but not RhoA signaling. Our findings indicate that RGS2 and RGS4 interact directly with PAR1 in $G\alpha$ -dependent manner to modulate PAR1/ $G\alpha$ -mediated signaling, and highlight a cellular mechanism for selective GPCR/G protein/RGS coupling.

Citation: Ghil S, McCoy KL, Hepler JR (2014) Regulator of G Protein Signaling 2 (RGS2) and RGS4 Form Distinct G Protein-Dependent Complexes with Protease Activated-Receptor 1 (PAR1) in Live Cells. PLoS ONE 9(4): e95355. doi:10.1371/journal.pone.0095355

Editor: Roland Seifert, Medical School of Hannover, Germany

Received: January 10, 2014; **Accepted:** March 26, 2014; **Published:** April 17, 2014

Copyright: © 2014 Ghil et al. This is an open-access article distributed under the terms of the Creative Commons Attribution License, which permits unrestricted use, distribution, and reproduction in any medium, provided the original author and source are credited.

Funding: This research was supported by an American Heart Association Pre-doctoral Fellowship Grant 0715465B (KLM), by the Basic Science Research Program through the National Research Foundation of Korea (NRF) funded by the Ministry of Education, Science and Technology (NRF-2012R1A1A2005207 to SG), and by grants from the National Institutes of Health (R01NS37112 and R01NS049195 awarded to JRH). The funders had no role in study design, data collection and analysis, decision to publish, or preparation of the manuscript.

Competing Interests: The authors have declared that no competing interests exist.

* E-mail: jhepler@emory.edu

Introduction

Extracellular signaling molecules such as neurotransmitters and hormones transmit their signals into cells by interacting with the large family (>900) of cell surface G protein coupled receptors (GPCRs) and linked heterotrimeric ($G\alpha\beta\gamma$ subunits) GTP binding proteins (G proteins). The binding of extracellular signaling molecules to GPCRs activate G proteins by inducing the exchange of GDP for GTP on the $G\alpha$ subunit. This facilitates $G\alpha$ -GTP dissociation from the $G\beta\gamma$ dimer and release of G proteins from the receptor [1]. Dissociated $G\alpha$ -GTP and $G\beta\gamma$ subunits interact with various downstream effectors and signaling pathways to mediate cell physiology. The life-time of this signaling event is dictated by the life-time of GTP bound to $G\alpha$, and is inactivated by the intrinsic GTPase activity characteristic of all $G\alpha$ subunits. However, $G\alpha$ GTPase activity is regulated and greatly accelerated by cofactor GTPase activating proteins (GAPs).

The most prominent GAPs for $G\alpha$ subunits include the family (~40 members) of regulators of G protein signaling (RGS) proteins, which bind to $G\alpha$ -GTP and increase GTP hydrolysis [2–4]. RGS proteins are classified into several subfamilies based on

their amino acid sequencing and protein structures [4,5], and are characterized by a shared RGS domain (~120 amino acid) that serves as the binding site for and confers the GAP activity onto $G\alpha$ -GTP. Recent studies have suggested that RGS proteins also can interact directly or indirectly with GPCRs [6–9]. RGS proteins interact with GPCR via the receptor third intracellular loops (i3), C-termini, or by recruiting adapter proteins to modulate the functions of coupled G proteins [9,10]. Therefore, compelling evidence indicates that GPCRs can selectively form a physical and functional complex with certain RGS protein and G proteins.

RGS proteins of the R4/B subfamily, including RGS1–5, 8, 13, 16, 18 and 21, are the smallest RGS proteins in size, each containing a single RGS domain with relatively small N and C-termini (except for RGS3) [5]. RGS2 is broadly expressed in both mouse and human tissues, and interacts with the $G_{q/11}$ family to inhibit $G_{q/11}$ -mediated signaling [11–13]. RGS2 also associates with several types of adenylyl cyclase and regulates intracellular cAMP concentration [14]. RGS4 is mainly expressed in brain and cardiac tissues [15,16], and interacts with $G\alpha_{i/o}$ and $G\alpha_q$ [11,17,18]. Previously, we reported that RGS2 and RGS4 can bind directly and selectively to GPCRs, to regulate the function of

linked G proteins. These interactions are regulated by specific regions with the N-termini of the RGS proteins and the i3 loops of the GPCRs [6,7].

Protease-activated receptors (PARs) are GPCRs that can be activated by proteases such as thrombin, trypsin and plasmin. Most GPCRs are activated by small hydrophilic molecules. By contrast, PARs are stimulated by proteolytic cleavage and binding of an intrinsic N-terminal ligand, which is cleaved by one or more endogenous proteases [19]. There exist four types of PARs termed PAR1-PAR4 in the order of their discovery. PAR1 was originally identified as a receptor for thrombin [20], and its functions have been widely studied in the cardiovascular and central nervous systems [21,22]. In our previous study, PAR1 was shown to form stable complexes with various G proteins including members of the G_{β} , G_q and G_{12} subfamilies. Stimulated PAR1 coupling to these G proteins induces activation of MAPK/ERK and inhibition of adenylyl cyclase ($G_{i/o}$), activation of inositol phosphate accumulation and calcium release ($G_{q/11}$), and activation of Rho activation ($G_{12/13}$ and $G_{q/11}$); PAR1 also stimulates migration of Neu7 glial cells [23,24].

A large body of evidence now exists to suggest that GPCRs and RGS proteins can form a physical and functional complex to regulate G protein signaling [9,10]. However what cellular factors dictate selective RGS/GPCR coupling is poorly understood. Most previous studies have used biochemical affinity pull-down assays to determine if RGS proteins can form a complex with GPCRs and/or G proteins. However, biochemical interactions such as these that depend on detergent extraction of receptors may not fully or accurately reflect functional GPCR/G protein/RGS protein complex formation in live cells. In addition, these studies have complicated experimental procedures. In the present study, we employed a bioluminescence resonance energy transfer (BRET) assay to investigate the mechanism whereby PAR1 and RGS proteins (RGS2 and RGS4) interact in live cells, in the presence or absence of G proteins. Here we report that PAR1 functionally interacts with both RGS2 and RGS4 in live cells, but only in a strict G protein-dependent manner to regulate PAR1/G protein signaling. Our findings suggest that both RGS2 and RGS4 each selectively modulate PAR1/ $G\alpha$ -mediated signaling by binding to PAR1 in a $G\alpha$ -dependent manner.

Materials and Methods

Construction of Plasmids

The mouse PAR1 cDNA (GenBank accession number NM_010169) in pBSK was a generous gift from Dr. Stephen Traynelis (Emory University). pcDNA3.1- $G\alpha_q$ YFP and - $G\alpha_s$ YFP plasmids were kindly provided by Dr. Joe Blumer (Medical University of South Carolina). pcDNA3.1- $G\alpha_q$, $G\alpha_{11}$ EE, - $G\alpha_i$, - $G\alpha_{oA}$ EE, - $G\alpha_{12}$ EE, - $G\alpha_{13}$ EE and - $G\alpha_s$ EE plasmids were obtained from Missouri S&T cDNA Resource Center. To generate PAR1-Ven plasmid (Venus-N1-PAR1, C-terminal Venus tagged plasmid of PAR1), PAR1 cDNA was amplified from pBSK-PAR1 by PCR with the primers 5'-ATC GAT AAG CTT GAT ATC GAA TTC-3' (forward), and 5'-TTT GGT ACC GCT AAT AGC TTT T-3' (reverse). The amplified products were inserted into the Venus-N1 using *HindIII* and *KpnI* restriction enzymes. Oligonucleotide primers used to create RGS2-Luc plasmid (pRLuc-N3-RGS2, C-terminal luciferase tagged plasmid of RGS2HA) are as follows: 5'-CTT GGT ACC ACC ATG CAA AGT GCT ATG TTC-3' (forward) and 5'-TTG GGC CCG AGC GTA ATC TGG AA-3' (reverse). pcDNA3.1-RGS2-HA was used as a template, and amplified PCR products were inserted into pRLuc-N3, using *KpnI* and *ApaI* restriction enzymes. RGS4-HA-

Luc plasmid (pRLuc-N3-RGS4, C-terminal luciferase tagged plasmid of RGS4-HA) were generated by PCR reaction with the primers, 5'-TTT AAA CTT AAG CTT GGT ACC ACC ATG TGC-3' (forward) and 5'-TTG GGC CCG AGC GTA ATC TGG AA-3' (reverse). pcDNA3.1-RGS4-HA was used as a template and amplified PCR products were inserted into pRLuc-N3 using *KpnI* and *ApaI* restriction enzymes. To make PAR1-FLAG plasmid (pcDNA3.1-PAR1-FLAG, C-terminal FLAG tagged plasmid of PAR1), PAR1 cDNA was amplified from pBSK-PAR1 by PCR with the primers, 5'-GAC GGT ATC GAT AAG CTT GAT ATC GAA TTC CCG GG-3' (forward) and 5'-AAA CTC GAG CTA CTT GTC ATC GTC GTC CTT GTA GTC AGC TAA TAG CTT T-3' (reverse). The amplified products were inserted into the pcDNA3.1 using *HindIII* and *XhoI* restriction enzymes. To generate a $G_{q/11}$ -insensitive mutant of PAR1 (R205A) [24] for BRET studies, the wild type mPAR1-Ven plasmid (above) was used as a template for amplification by QuickChange (QIAGEN) using primers, 5'-CAT AAG CAT TGA CGC GTT CCT GGC GGT G-3' (forward) and 5'-CAC CGC CAG GAA CGC GTC AAT GCT TAT G-3' (reverse). The amplified product was then digested with *DpnII* to remove the parent DNA, transformed into bacterial strain XL-Blue, and DNA recovered from resulting colonies was sequenced to confirm insertion of mutant R205A.

Cell Culture and Transfection

The COS7 cell line (American Type Culture Collection, ATCC, CRL 1651) was maintained in DMEM (without phenol red) supplemented with 10% fetal bovine serum, 2 mM glutamine, 100 units/ml penicillin, and 100 μ g/ml streptomycin. Cells were incubated at 37°C with 5% CO₂ in a humidified incubator. Cells were transiently transfected with the indicated plasmids using lipofectamine 2000, following the manufacturer's instructions.

BRET Assays

BRET assays were performed in the same manner as has been previously described [25,26]. Briefly, COS7 cells were transfected with BRET donor (luciferase-tagged) and acceptor (Venus-tagged) plasmids. After 48 h, cells were washed with PBS and harvested with Tyrode's solution (140 mM NaCl, 5 mM KCl, 1 mM MgCl₂, 1 mM CaCl₂, 0.37 mM NaH₂PO₄, 24 mM NaHCO₃, 10 mM HEPES, and 0.1% glucose, pH 7.4). Cells were distributed in triplicate at 1×10^5 cells/well into gray 96-well OptiPlates (PerkinElmer Life Science). Venus-tagged protein expression levels were measured by using TriStar LB941 plate reader (Berthold Technologies) with excitation and emission filters at 485 nm and 535 nm, respectively. To measure BRET signals, the cells were treated with luciferase substrate, coelenterazine H (Nanolight Technology, final concentration 5 μ M). After 2 min, the luminescence was measured by using 480 \pm 20 and 530 \pm 20 nm filters. BRET signals were determined by calculating the ratio of the light intensity emitted by the Venus divided by the light intensity emitted by luciferase. Net BRET values were corrected by subtracting the background BRET signal detected from expression of the Luciferase alone. The expression levels of $G\alpha$ protein were determined by immunoblot, using antibodies against $G\alpha_q$, $G\alpha_{11}$, $G\alpha_o$, $G\alpha_{12}$ (all $G\alpha$ antibodies from Santa Cruz Biotechnology) and EE-epitope tag (Covance).

Generation and Purification of GST-PAR1 Intracellular Loop Fusion Proteins

cDNA encoding glutathione-S-transferase (GST)-PAR1-i2, GST-PAR1-i3, and GST-PAR1-i3 were cloned into the pGEX4T

vector. For this, the second intracellular loop (i2 loop) or the i3 loop of PAR1 was each amplified by PCR from corresponding regions of the mouse full-length receptor including *EcoRI* and *XhoI* cut site as linkers. These fragments were cloned in frame of the pGEX4T vector (*EcoRI/XhoI*) encoding an N-terminal GST tag.

For protein production, plasmid constructs encoding GST-PAR1 i2 and i3 loop fusion proteins were transformed into *E. coli* strain BL21/DE3 for 2 h at 37°C with shaking. Cells were centrifuged, and pellets were frozen at -80°C. Pellets were thawed in harvest buffer (10 mM HEPES pH 8, 50 mM NaCl, 5 mM EDTA, 0.5% Triton-X100) supplemented with protease inhibitors and lysozyme, sonicated, and then centrifuged at 4°C to yield bacterial cell lysates. Lysates were combined and mixed with Glutathione-sepharose 4B beads (Amersham-Pharmacia) for 1 h, at 4°C. Protein-bead complexes were recovered and then washed with harvest buffer, and stored as slurry solutions in harvest buffer at -80°C until experimentation. The protein concentration present in the slurries was determined by Coomassie blue staining versus BSA standards, and the same amount of total protein was used for in each binding reaction.

RGS Affinity Pull-down Assays

RGS protein affinity pull-down assays were performed as previously described [6,7]. Briefly, Glutathione-sepharose 4B beads containing equal amounts of GST-PAR1-i2 or GST-PAR1-i3 fusion proteins (above) were mixed with equal amounts of purified His-tagged RGS proteins in a total reaction volume of 250 μ L of reaction buffer (30 mM Imidazole and 80 mM NaCl, 10 mM HEPES, pH 7.4 final to minimize non-specific binding), and reactions were mixed overnight at 4°C. Beads were pelleted by centrifugation and were washed with harvest buffer. Proteins bound to the beads were eluted with 2X sample buffer and were detected by immunoblot.

Measurement of Erk Activation in Cells

COS-7 cells were transiently transfected with empty vector (pcDNA3.1), vector encoding PAR1 alone, or PAR1 together with vector encoding C-terminally HA-tagged RGS2 (RGS2-HA), RGS4-HA, or RGS16-HA. After overnight serum starvation, cells were stimulated with 20% serum (positive control) or with PAR1 peptide agonist (30 μ M TFLLR) for 2–5 min, harvested, sonicated, boiled in sample buffer, subjected to Western blot analysis with p44/42 ERK1/2 and phospho-p44/42 ERK1/2 antibodies (Cell Signaling Technology) at 4°C. Detection of the HA-tagged RGS proteins was performed by immunoblotting the same samples used in the ERK1/2 phosphorylation experiments.

Measurement of Calcium Signaling in *Xenopus Laevis* Oocytes by Two-electrode Voltage Clamp Recordings

Oocytes were harvested from *X. laevis* were defolliculated and maintained in 1x Barth's culture solution at 16°C. Stage V–VI oocytes were either injected with 5 ng PAR1 cRNA, which was synthesized from cDNA according to the manufacturer's specifications (Ambion). Recordings were performed 4–5 days after injections. The recording solution contained 60 mM NaCl, 38 mM KCl, 2.3 mM CaCl₂, 1 mM MgCl₂, and 6 mM HEPES (pH 7.4). Patch pipettes with tip diameters of 1–2 μ m were used as electrodes and filled with 300 mM KCl. Current responses were recorded at a holding potential of -40 mV. Data was acquired and voltage was controlled with a two-electrode voltage-clamp amplifier (OC-725; Warner Instruments). PAR1-agonist peptide TFLLR was diluted in 1x Barth's to final concentrations of 30 μ M and was used to elicit the ICl (Ca). For studies with RGS protein

regulation of PAR1 signaling, 5 ng cRNA for each RGS was added with 5ng PAR1 cRNA prior to injection. Recordings were performed 4–5 days after injections as detailed above.

Measurement of RhoA Activation

The GTP-bound form of RhoA was measured using the absorbance-based RhoA Activation G-LISA kit (Cytoskeleton Inc.) according to the manufacturer's protocol. COS-7 cells were transiently transfected with cDNA encoding empty vector (control) or with vector encoding C-terminally HA-tagged RGS2 (RGS2-HA), RGS4-HA or RGS16-HA. Prior to assay, transfected COS-7 cells were serum-starved overnight and then treated for 2 min with TFLLR. The absorbance from the G-LISA plate was read by a spectrophotometer at a wavelength of 490 nm.

Results

1. Interaction between PAR1 and RGS2 in Live Cells

Previous reports indicate that some RGS proteins interact directly with GPCRs to modulate their signals [9,10]. To determine whether RGS2 interacts with PAR1 in live cells, we performed BRET assays using PAR1-Venus (PAR1-Ven) and RGS2-Luciferase (RGS2-Luc) plasmids. As a negative control, we used RGS14-Luc, which we recently reported interacts with the α 2-adrenergic receptors in cells using BRET assays [25,26]. In COS7 cells transfected with PAR1-Ven and a fixed amount of RGS2-Luc as donor (35 ng), the BRET signals increased with increasing amounts of PAR1 acceptor, whereas no BRET signals were detected between PAR1-Ven and RGS14-Luc (Fig. 1A). In the presence of the PAR1 peptide agonist TFLLR, the BRET signals between PAR1-Ven and RGS2-Luc were increased compared with no agonist. RGS2 is coupled with G_{q/11} family, and inhibits their functions [11,12]. To investigate the dependency of PAR1·RGS2 interaction on the presence of G_{q/11}, we co-transfected cells with untagged G α _q or G α ₁₁ together with PAR1-Ven and RGS2-Luc. Expression of G α _q or G α ₁₁ significantly increased the interaction between acceptor and donor, and this signal was marginally enhanced by the addition of TFLLR (Fig. 1B and C). We next tested the effect of other G α subunits on PAR1·RGS2 interaction and observed that the BRET signals were not altered in the presence of G α _{i/o}, G α _{12/13} or G α _s (Fig. 1D and Fig. S1). Taken together, these results indicate that RGS2 can interact with PAR1 in live cells, and that their interaction is markedly promoted by the presence of either G α _q or G α ₁₁ and by receptor agonist, but not by other Ga subunits.

To further explore if receptor/G α _q coupling promotes interaction between PAR1 and RGS2, we co-transfected G α _q-YFP, RGS2-Luc and/or PAR1-FLAG, and the cells were subjected to the BRET assay. G α _s-YFP was used as a negative control. As before, BRET signals between G α _q-YFP and RGS2-Luc were increased by the expression of PAR1-FLAG (Fig. 2A) and further increased by the PAR1 agonist TFLLR. By contrast, no BRET signals were observed with G α _s-YFP (Fig. 2A). We previously reported that mutation of a single arginine residue of PAR1 (PAR1^{R205A}) disrupted binding to and functional coupling with G α _{q/11} [24]. We investigated the effects of PAR1^{R205A} on complex formations with RGS2 and G α ₁₁. Whereas the PAR1^{R205A} mutant can still interact weakly with RGS2 similar to wild type PAR1, this binding was not further enhanced by G α ₁₁ (Fig. 2B), indicating that the PAR1/G α _{q/11} complex is a preferred substrate for RGS2 in live cells.

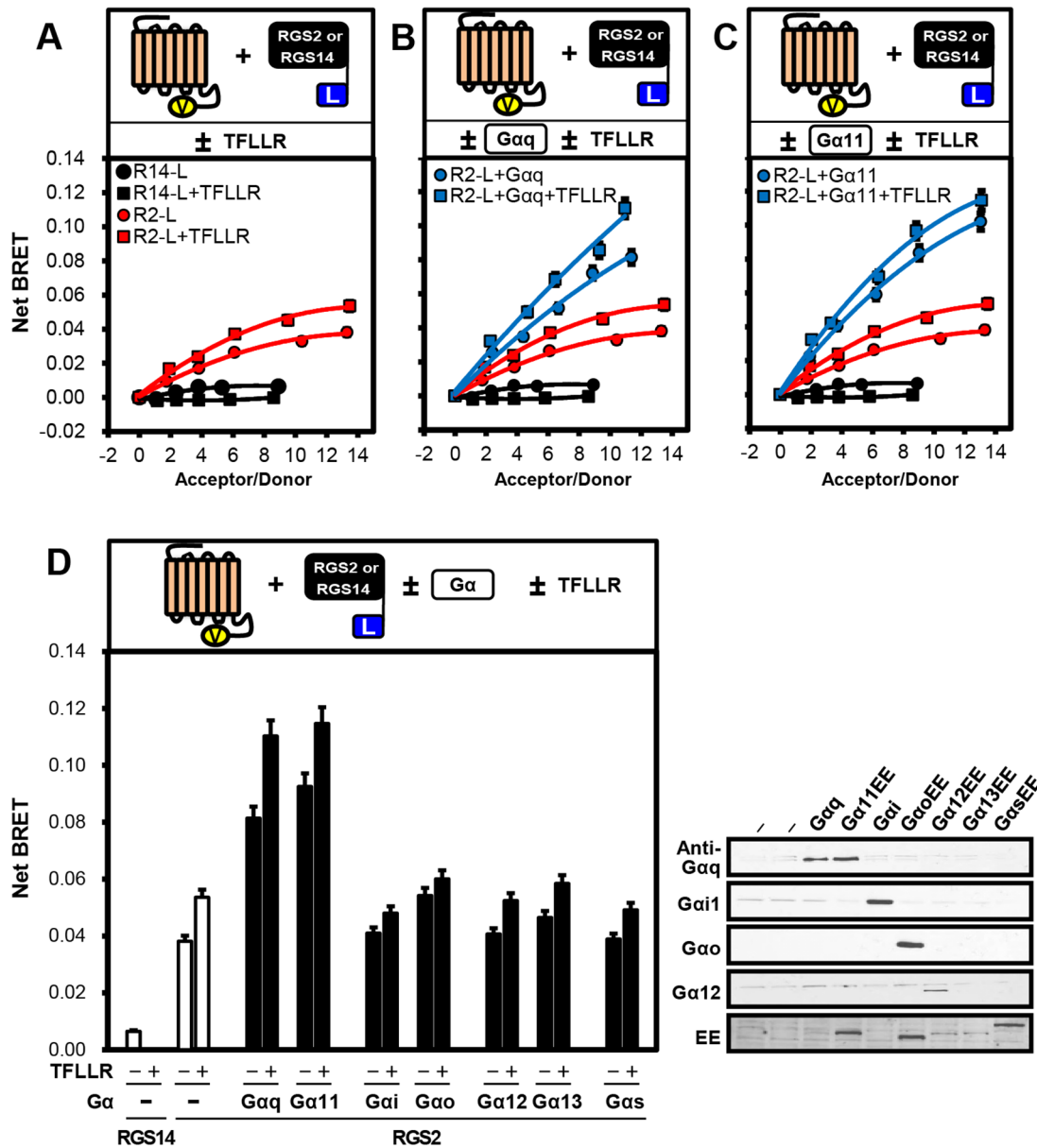


Figure 1. RGS2 interacts with PAR1 in live cells. **A**, Top panel: Cartoon illustrating proteins and conditions used in the experiment. Bottom panel: COS7 cells transfected with an increased amount of PAR1-Ven (0, 0.25, 0.5, 1.0, 1.5, 2.0 μ g), together with a fixed amount of RGS2-Luc (35 ng) or RGS14-Luc (5 ng), were subjected to the BRET assay in both the absence and presence of 30 μ M of TFLLR. Net BRET signals are shown between PAR1-Ven and either RGS2-Luc or RGS14-Luc. **B** and **C**, Top panel: Cartoons illustrating proteins and conditions used in the experiment. Bottom panel: COS7 cells transfected with an increased amount of PAR1-Ven, together with fixed amount of RGS2-Luc or RGS14-Luc, were subjected to the BRET assay in both the absence and presence of untagged $G\alpha_q$ (B), $G\alpha_{11}$ (C) and TFLLR. Bottom panel, net BRET signals are shown between PAR1-Ven and either RGS2-Luc or RGS14-Luc. The black and red plots in (B) and (C) were identical to those in (A). **D**, Top panel: Cartoon illustrating proteins and conditions used in the experiment. Bottom panel: COS7 cells were transfected with both fixed amount of PAR1-Ven (2.0 μ g) and either RGS2-Luc (35 ng) or RGS14-Luc (5 ng), and the cells were subjected to the BRET assay in both the absence and presence of 0.5 μ g of untagged $G\alpha$ and TFLLR. Bottom panel, net BRET signals are shown between PAR1-Ven and either RGS2-Luc or RGS14-Luc. Right panel, shows a representative immunoblot of the different untagged $G\alpha$ subunits used in the BRET experiment. All BRET graphs are representative of at least three independent experiments. Abbreviations: R14-L, RGS14-Luc; R2-L, RGS2-Luc. doi:10.1371/journal.pone.0095355.g001

2. Interaction between PAR1 and RGS4 in Live Cells

Like RGS2, RGS4 binds directly to GPCRs, including opioid receptors, and modulates their functions [8]. Therefore, to investigate whether RGS4 binds to PAR1 here in live cells, we co-transfected with PAR1-Ven and RGS4-Luc, and the cells were subjected to the BRET assay. Unlike RGS2 (Fig. 1A), RGS4 had weak binding properties to PAR1 in the absence of $G\alpha$ in live cells

(Fig. 3A). However, high levels of BRET activity were observed only in the presence of $G\alpha_o$ (Fig. 3B and C), with lower signals evident with $G\alpha_i$, and even less BRET activity with $G\alpha_q$, $G\alpha_{11}$, $G\alpha_{12}$, $G\alpha_{13}$ and $G\alpha_s$ (Fig. 3C and Fig. S2), suggesting that PAR1 binding to RGS4 may be $G\alpha_o$ -dependent.

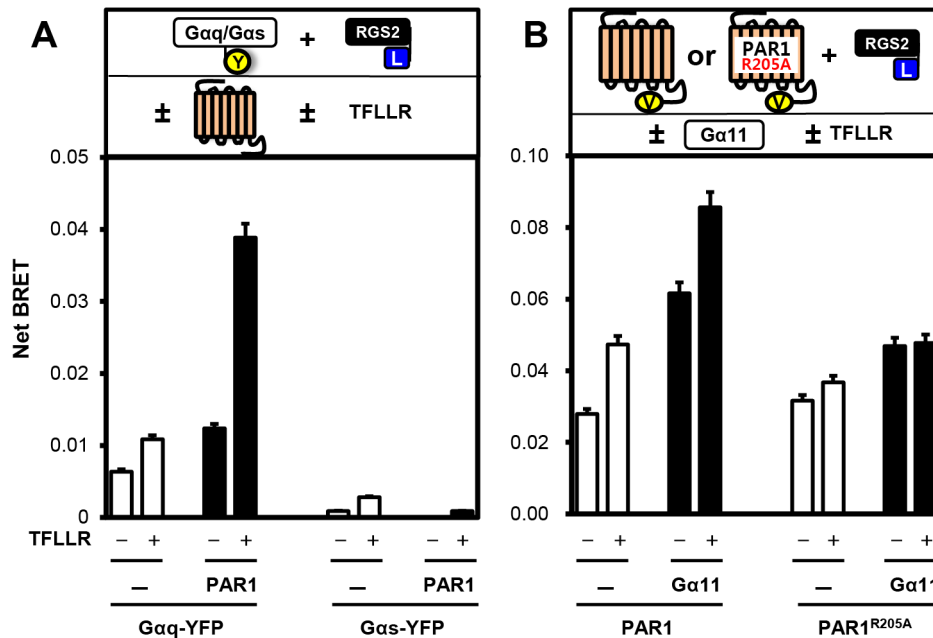


Figure 2. PAR1 forms a complex with RGS2 and $G_{\alpha q/11}$. **A**, Top panel: Cartoon illustrating proteins and conditions used in the experiment. Bottom panel: COS7 cells transfected with RGS2-Luc (35 ng) and either $G_{\alpha q}$ -YFP or $G_{\alpha s}$ -YFP (0.75 μ g) were subjected to the BRET assay in both the absence and presence of 0.5 μ g of untagged PAR1-FLAG and 30 μ M of TFLLR. Net BRET signals are shown between RGS2-Luc and either $G_{\alpha q}$ -YFP or $G_{\alpha s}$ -YFP. **B**, Top panel, Cartoon illustrating proteins and conditions used in the experiment. Bottom panel: COS7 cells transfected with RGS2-Luc (35 ng) and either PAR1-Ven or PAR1^{R205A}-Ven (1.5 μ g) were subjected to the BRET assay in both the absence and presence of 0.5 μ g of untagged $G_{\alpha 11}$ and TFLLR. Net BRET signals are shown between RGS-Luc and either PAR1-Ven or PAR1^{R205A}-Ven. doi:10.1371/journal.pone.0095355.g002

3. RGS2 and RGS4 Bind Directly, and Selectively to the i3 Loop of PAR1

To determine whether PAR1 binds directly to the RGS2 and RGS4, and consequently which domain of PAR1 might be the main contributor to binding of the RGS proteins, we purified His-tagged RGS proteins (RGS1-His, RGS2-His, RGS4-His and RGS16-His), and GST-tagged PAR1-i2 and -i3 domains from a bacterial culture, and performed a GST-affinity pull-down assays. RGS2 and RGS4, but not RGS1 or RGS16 bound robustly to the PAR1 i3 loop but not GST. By comparison, RGS2, RGS4 and RGS16 bound only weakly to the i2 loop (compared to GST alone) and RGS1 did not bind to either PAR1 i2 or i3 (Fig. 4A and B).

4. Effect of RGS2 and RGS4 on PAR1- G_{α} -Mediated Signaling

PAR1 relies upon $G_{\alpha q/11}$ to activate PLC- β and linked intracellular $InsP_3$ -calcium signaling [23,24]. Therefore, to determine whether RGS2 and RGS4 inhibit PAR1-directed $G_{\alpha q/11}$ signaling, we measured the capacity of RGS2 and RGS4 to modulate calcium-activated chloride channels in *Xenopus* oocytes. Our previous studies showed that RGS4 blocks a chloride channel current in *Xenopus* oocytes that is activated by a GPCR/ $G_{\alpha q/11}$ / $Ins(1,45)P_3$ /calcium pathway, and that RGS4 acts by blocking G_q /calcium signaling but does not directly affect chloride channel function [27]. In the presence of TFLLR, PAR1 activated the calcium-dependent chloride channel and expression of either RGS2 or RGS4 but not RGS1 each completely blocked this PAR1- $G_{\alpha q/11}$ -stimulated chloride current (Fig. 5A), indicating that RGS2 and RGS4 inhibit PAR1- $G_{\alpha q/11}$ -mediated calcium signaling. We next tested if RGS2 or RGS4 regulates PAR1- G_{α} stimulated MAPK/ERK signaling. GPCR activation generally

stimulates MAPK/ERK signaling through multiple G protein-mediated signaling cascades [28]. In our previous study, PAR1 activation was shown to induce MAPK/ERK phosphorylation, and this effect is completely blocked by PTX, indicating PAR1 can stimulate MAPK/ERK signaling in a $G_{i/o}$ -dependent manner [23]. To investigate whether RGS2 and RGS4 inhibit MAPK/ERK phosphorylation, the MAPK/ERK phosphorylation assay was performed by using phospho-ERK antibodies. We transfected PAR1 and either HA-tagged RGS2, RGS4 or RGS16 in COS7 cells, and activated the receptors using TFLLR. Fig. 5B shows that expression of either RGS2 or RGS4 inhibits MAPK/ERK phosphorylation to some extent, whereas no effect was observed with RGS16 indicating that MAPK/ERK signaling induced by PAR1/ G protein is limited by RGS2 and RGS4.

Signaling through the $G_{12/13}$ family transduces GPCR signals into RhoA activation, actin remodeling, and assembly of focal adhesions [29,30]. In addition, PAR1 uses $G_{12/13}$ family to activate RhoA as we have previously reported [23]. To elucidate whether RGS2 and RGS4 inhibit PAR1/ G_{12} -mediated Rho signaling, we performed Rho activity assay in COS7 cells transfected with PAR1 alone, or together with HA-tagged RGS2, RGS4 or RGS16. Even when RGS proteins were highly expressed in the cells, RhoA activation was not altered compared to PAR1 alone, indicating that RGS2 and RGS4 do not affect PAR1/ $G_{12/13}$ -mediated RhoA signaling (Fig. 5C). Taken together, these data suggest that RGS2 and RGS4 selectively inhibit PAR1/ G_{α} -mediated signaling.

Discussion

In this study, we investigated whether RGS2 and RGS4 interact with PAR1 receptors in live cells, and we also determined whether their interaction affected PAR1/ G_{α} -mediated signaling. Our

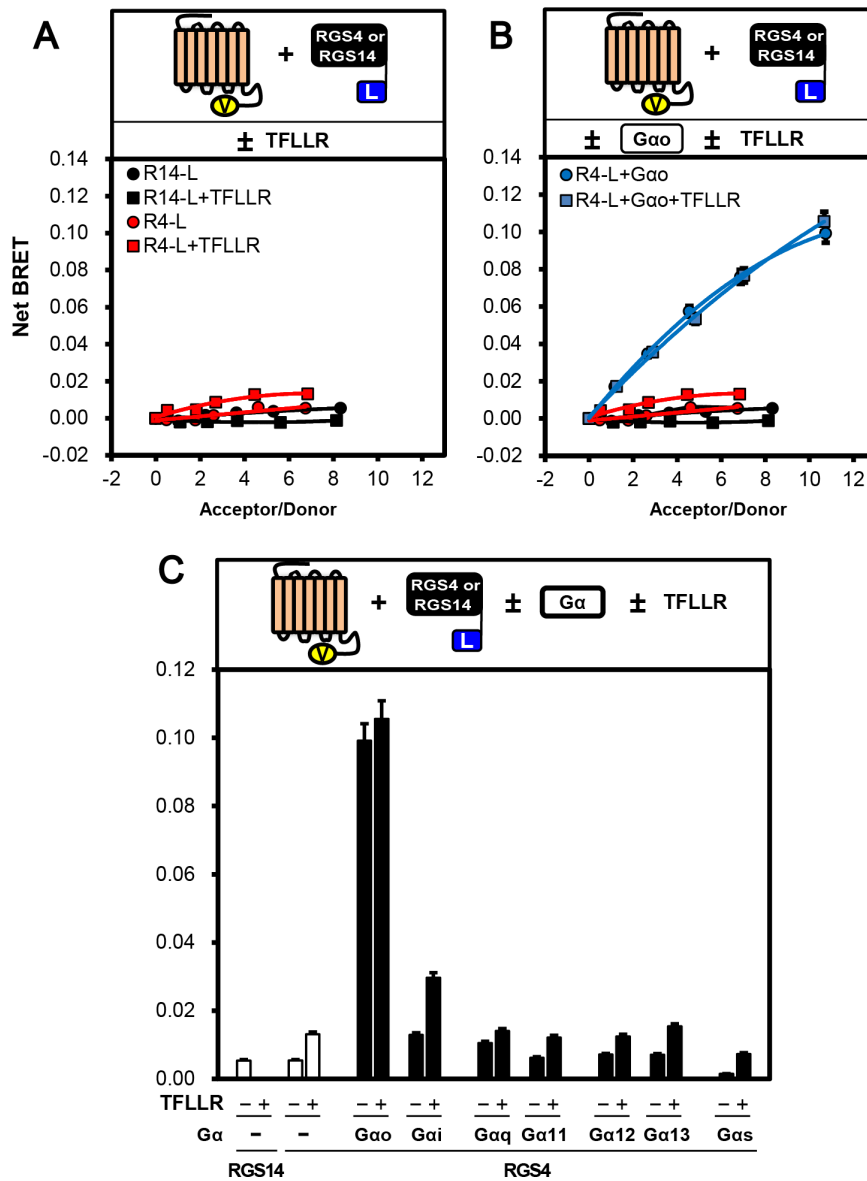


Figure 3. RGS4 interacts with a PAR1/G α_o complex in live cells. **A**, Top panel: Cartoon illustrating proteins and conditions used in the experiment. Bottom panel: COS7 cells were transfected with increasing amounts of PAR1-Ven (0, 0.1, 0.25, 0.5, 1.0, 1.5 μ g), together with fixed amount of RGS4-Luc (45 ng) (Red symbols) or RGS14-Luc (5 ng) (Black symbols), and the cells were subjected to BRET analysis in both the absence and presence of 30 μ M of TFLLR. Net BRET signals are shown between PAR1-Ven and either RGS4-Luc or RGS14-Luc. **B**, Top panel: Cartoon illustrating proteins and conditions used in the experiment. Bottom panel: COS7 cells were transfected with an increasing amount of PAR1-Ven together with fixed amount of RGS4-Luc (Red symbols) or RGS14-Luc (Black symbols) as in A, and were subjected to BRET analysis in both the absence or presence of untagged G α_o (Blue symbols) and TFLLR. Net BRET signals are shown between PAR1-Ven and either RGS4-Luc or RGS14-Luc. (NOTE: The black and red plots in (B) were identical to those in (A)). **C**, Top panel: Cartoon illustrating proteins and conditions used in the experiment. Bottom panel: COS7 cells were transfected with both fixed amount of PAR1-Ven (1.5 μ g) and either RGS4-Luc (45 ng) or RGS14-Luc (5 ng), and the cells were subjected to the BRET assay in both the absence and presence of 0.5 μ g of untagged G α and TFLLR. Net BRET signals are shown between PAR1-Ven and either RGS4-Luc or RGS14-Luc. Abbreviations used are R14-L = RGS14-Luc; R4-L = RGS4-Luc. doi:10.1371/journal.pone.0095355.g003

findings (Fig. 1–4) show that RGS2 and RGS4 interacted with PAR1 in live cells in a G α -dependent manner, and that these interactions may be direct. RGS2 selectively formed a complex with PAR1 and G $\alpha_{q/11}$, whereas RGS4 selectively formed a complex with PAR1 in the presence of G α_o . Figure 5 shows that PAR1-G α -mediated calcium and MAPK/ERK signaling was inhibited by RGS2 and RGS4. Although PAR1 couples with G $\alpha_{12/13}$ family and increases RhoA activity in the presence of TFLLR [23], RGS2 and RGS4 did not alter the PAR1/G α_{12} -mediated

RhoA activation in the presence of TFLLR. This may be due to the fact RGS2 and RGS4 preferentially interact with G α_q and G α_i /G α_{11} family members, respectively [11,12].

It is well established that RGS2 selectively binds to G $\alpha_{q/11}$ to inhibit their signaling [11]. However, low levels of BRET signals between G α_q -YFP and RGS2-Luc were displayed in the absence of PAR1 and TFLLR (Fig. 2A). The RGS homology domain of RGS proteins interacts with the “switch” region located within the alpha helical domains of G α [31,32]. The coding sequence of YFP

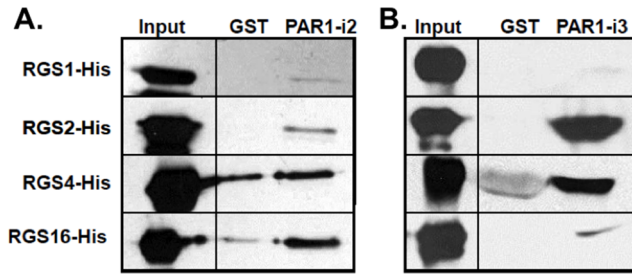


Figure 4. RGS2 and RGS4 bind directly and selectively to the i3 loop of PAR1. Purified RGS1-His, RGS2-His, RGS4-His or RGS16-His were incubated with equal amounts of GST alone, GST-PAR1-i2, or with GST-PAR1-i3 bound to glutathione-Sepharose beads. After centrifugation, bound RGS proteins were eluted in 2X sample buffer and subjected to SDS-PAGE. Immunoblots were performed using an anti-His antibody.
doi:10.1371/journal.pone.0095355.g004

in G_{α_q} -YFP was inserted in the alpha helical domain (αb - αc loop) of G_{α_q} [33,34]. We consider the possibility that insertion of YFP in G_{α_q} might cause a change of G_{α_q} protein conformation, so as to decrease affinity with RGS2. However, the BRET signals between G_{α_q} -YFP and RGS2-Luc were increased in the presence of untagged PAR1 and TFLLR (Fig. 2A), indicating that activation of PAR1 can induce conformational change of both proteins and, as a result, induce formation of a PAR1· G_{α_q} -YFP·RGS2-Luc protein complex.

GPCRs are integral membrane proteins that possess seven-transmembrane domains. They contain three extracellular loops and three (or in some cases four) intracellular loops. Intracellular loops contribute to direct interaction with various signaling and regulatory proteins including many of G proteins, RGS proteins, arrestins, kinases, cytoskeletal-associated proteins, and other GPCRs [35]. The second intracellular (i2) loop of PAR1

contributes to G_{α} coupling [24,36]. The Arg-205 residue in the i2 loop of PAR1 plays a pivotal role in the binding of $G_{\alpha_{q/11}}$ and transduction of $G_{\alpha_{q/11}}$ -mediated signaling [24]. In Figure 2B, the PAR1^{R205A}-Ven mutant failed to stimulate BRET signals in the presence of $G_{\alpha_{11}}$. As a result, we can confirm that $G_{\alpha_{q/11}}$ plays a crucial role in the induction of PAR1·RGS2 complex formation. Moreover, our results (Fig. 4) suggest that i3 loops of PAR are necessary for binding to RGS2 and RGS4. Taken together, the i2 and i3 loops of PAR1 mainly contribute to binding to $G_{\alpha_{11}}$ and RGS2, respectively.

Like RGS2, RGS4 can bind to both G_i and G_q families and prohibit G_{α} -related GPCR pathways [11,17,18,37]. Interestingly, we found that only G_{α_o} can stimulate BRET signals between PAR1-Ven and RGS4-Luc (Fig. 3). Although G_{α_i} shares high sequence identity with G_{α_o} , we find that G_{α_i} failed to alter BRET signals. Evidence suggests that G_{α_o} has a function distinct from G_{α_i} . G_{α_o} binds directly to the catalytic subunit of PKA, and interferes with nuclear translocation of PKA [38]. Activation of G_{α_o} , but not G_{α_i} , is sufficient to promote neuritogenesis by modulating RapGAP activity in Neuro2A neuroblastoma cells [39,40]. Therefore, G_{α_o} seems to have functions distinct from G_{α_i} . PAR1 can couple to multiple G proteins from different G protein families raising the possibility that other G_{α_i} family members may recruit specific RGS proteins to PAR1 [23]. PAR1 couples most robustly to G_{α_o} and this interaction may selectively recruit RGS4 to PAR1 for distinct functions as well [23].

In our previous study, PAR1-induced MAPK/ERK activation was completely blocked by PTX in COS7 cells [23], indicating that this activity is primarily mediated by the $G_{i/o}$ family. We find that RGS2 and RGS4 each inhibited PAR1-mediated MAPK/ERK signaling pathway (Fig. 5) suggesting that these RGS proteins prohibited PAR1/ G_{α} -mediated MAPK/ERK signaling. In addition, both RGS2 and RGS4 inhibited PAR1/ $G_{\alpha_{q/11}}$ -mediated calcium signaling, but not PAR1/ $G_{\alpha_{12/13}}$ -mediated Rho signaling. Our BRET studies here indicate that RGS2 and

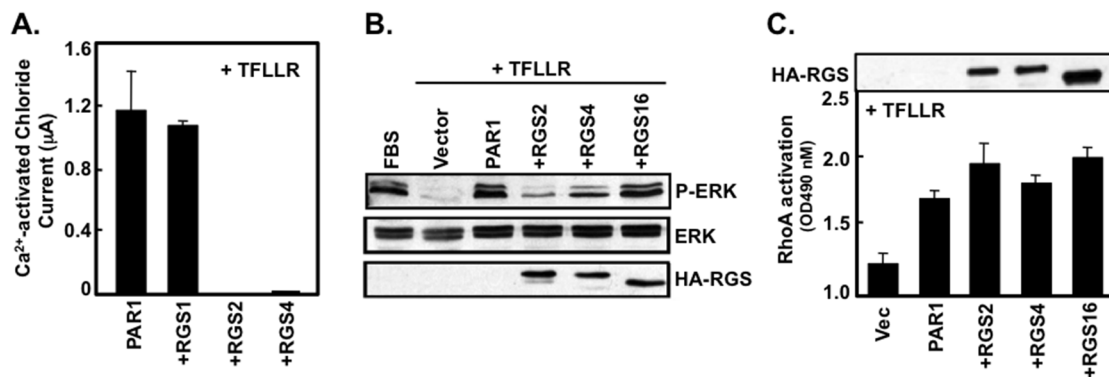


Figure 5. RGS2 and RGS4 selectively inhibit PAR1/ G_{α} -mediated signaling in live cells. **A**, RGS2 and RGS4, but not RGS1, reduce PAR1-evoked calcium activated chloride currents in oocytes. PAR1 cRNA alone or mixed with individual RGS protein cRNA was injected into *X. laevis* oocytes, which were sustained in 1x Barth's solution. 4–5 days after injection, Ica (Cl) measurements were obtained from the oocytes in response to activation with 30 mM TFLLR. A two electrode voltage clamp was used to obtain the current changes, as described in Materials and Methods. Data were entered into a Microsoft Excell spreadsheet which was used to calculate the mean change in Ica (Cl) + S.E.M. ($n \geq 11$ oocytes). **B**, RGS2 and RGS4 differentially block PAR1-stimulated ERK1/2 phosphorylation. Vector alone or PAR1 alone, or pairs of PAR1 and the indicated RGS protein were separately transfected into COS-7 cells. Cells were either stimulated with 20% serum or 30 μ M TFLLR for 5 min. Immunoblots were performed with either phospho-ERK1/2, total ERK1/2, or an anti-HA antibody, followed by a goat-anti rabbit secondary antibody and detected by ECL. **C**, PAR1-mediated RhoA activation is not regulated by RGS proteins. As described in the materials and methods section, RhoA activation was measured using a RhoA G-LISA Assay kit. Vector alone, PAR1 alone, or PAR/RGS pairs were separately transfected into COS-7 cells for 5 h before an overnight period of serum starvation. The next day, cells were stimulated with 30 μ M TFLLR for 2 min prior to cell lysis. The manufacturer's protocol was followed throughout the experiment, and the absorbance of each well was read with a spectrophotometer wavelength of 490 nm. Data were entered into a Microsoft Excel spreadsheet which was used to calculate the mean fold change in absorbance (bars) over basal levels plus the S.E.M (error bars), $n = 3$ for each condition.
doi:10.1371/journal.pone.0095355.g005

RGS4 bind to $G\alpha_{q/11}$ and to $G\alpha_o$, respectively, to form functional complexes with PAR1. Taken together, our findings suggest that PAR1/ $G_{q/11}$ recruits RGS2 to mediate calcium signaling, and that PAR1/ $G_{i/o}$ recruits RGS4 to mediate MAPK/ERK signaling, although we note that RGS2 and RGS4 may also suppress MAPK/ERK signaling calcium signaling, respectively, by binding G proteins directly independent of PAR1.

In summary, we observed the binding properties between PAR1, $G\alpha$ and RGS proteins, including RGS2 and RGS4 in live cells, and we also tested whether RGS2 and RGS4 inhibit the PAR1/ $G\alpha$ -mediated signaling pathway. RGS2 and RGS4 selectively bind to and inhibit PAR1/ $G_{q/11}$ - and PAR1/ $G_{i/o}$ -mediated signals, respectively, and there is a difference in the binding properties of RGS proteins with PAR1 depending on the $G\alpha$. Our findings are consistent with a very recent report showing that PAR1 signaling is modulated by R4 family members of RGS proteins that include RGS2 and RGS4 [41], and provide new insights into molecular mechanisms for how GPCR, RGS and $G\alpha$ form functional preferred signaling complexes within cells. These studies could be of value in developing small molecule modulators of PAR1 signaling pathways.

Supporting Information

Figure S1 COS7 cells transfected with an increased amount of PAR1-Ven (0, 0.25, 0.5, 1.0, 1.5, 2.0 μ g) together with a fixed amount of RGS2-Luc (35 ng) (Red symbols) or RGS14-Luc (5 ng) (Black symbols) were subjected to the BRET assay in both the absence and presence of 0.5 μ g of $G\alpha$ (Blue symbols) [$G\alpha_i$ (A), $G\alpha_o$ (B), $G\alpha_{12}$ (C), $G\alpha_{13}$ (D) and $G\alpha_s$ (E)], and 30 μ M of TFLLR. Net

BRET signals are shown between PAR1-Ven and either RGS2-Luc or RGS14-Luc. The black and red data and plots in (B) – (E) were identical to those in (A). Abbreviations used are R14-L = RGS14-Luc; R2-L = RGS2-Luc. (TIF)

Figure S2 COS7 cells were transfected with an increased amount of PAR1-Ven (0, 0.1, 0.25, 0.5, 1.0 and 1.5 μ g) together with fixed amount of RGS4-Luc (45 ng) (Red Symbols) or RGS14-Luc (5 ng) (Black Symbols), and the cells were subjected to the BRET assay in both the absence and presence of 0.5 μ g of $G\alpha$ (Blue symbols) [$G\alpha_i$ (A), $G\alpha_q$ (B), $G\alpha_{11}$ (C), $G\alpha_{12}$ (D), $G\alpha_{13}$ (E), and $G\alpha_s$ (F)] and 30 μ M of TFLLR. Net BRET signals are shown between PAR1-Ven and either RGS4-Luc or RGS14-Luc. The black and red data and plots in (B) – (F) were identical to those in (A). Abbreviations used are R14-L = RGS14-Luc; R4-L = RGS4-Luc. (TIF)

Acknowledgments

The authors would like to thank Suneela Ramineni for outstanding technical assistance, and Dr. Stephen F. Traynelis for opening his lab and assisting with the *X. laevis* oocyte electrophysiology recordings.

Author Contributions

Conceived and designed the experiments: SG KLM JRH. Performed the experiments: SG KLM JRH. Analyzed the data: SG KLM JRH. Contributed reagents/materials/analysis tools: SG KLM JRH. Wrote the paper: SG JRH. Edited the manuscript: SG JRH.

References

- Hepler JR, Gilman AG (1992) G proteins. Trends Biochem Sci 17: 383–387.
- He W, Cowan CW, Wensel TG (1998) RGS9, a GTPase accelerator for phototransduction. Neuron 20: 95–102.
- Ross EM, Wilkie TM (2000) GTPase-activating proteins for heterotrimeric G proteins: regulators of G protein signaling (RGS) and RGS-like proteins. Annu Rev Biochem 69: 795–827.
- Hollinger S, Hepler JR (2002) Cellular regulation of RGS proteins: modulators and integrators of G protein signaling. Pharmacol Rev 54: 527–559.
- Bansal G, Druey KM, Xie Z (2007) R4 RGS proteins: regulation of G-protein signaling and beyond. Pharmacol Ther 116: 473–495.
- Bernstein LS, Linder ME, Hepler JR (2004) Analysis of RGS protein palmitoylation. Methods Mol Biol 237: 195–204.
- Hague C, Bernstein LS, Ramineni S, Chen Z, Minneman KP, et al. (2005) Selective inhibition of alpha1A-adrenergic receptor signaling by RGS2 association with the receptor third intracellular loop. J Biol Chem 280: 27289–27295.
- Georgoussi Z, Leontiadis L, Mazarakou G, Merkouris M, Hyde K, et al. (2006) Selective interactions between G protein subunits and RGS4 with the C-terminal domains of the mu- and delta-opioid receptors regulate opioid receptor signaling. Cell Signal 18: 771–782.
- Neitzel KL, Hepler JR (2006) Cellular mechanisms that determine selective RGS protein regulation of G protein-coupled receptor signaling. Semin Cell Dev Biol 17: 383–389.
- McCoy KL, Hepler JR (2009) Regulators of G protein signaling proteins as central components of G protein-coupled receptor signaling complexes. Prog Mol Biol Transl Sci 86: 49–74.
- Heximer SP, Watson N, Linder ME, Blumer KJ, Hepler JR (1997) RGS2/G0S8 is a selective inhibitor of Gqalpha function. Proc Natl Acad Sci U S A 94: 14389–14393.
- Heximer SP, Srinivasa SP, Bernstein LS, Bernard JL, Linder ME, et al. (1999) G protein selectivity is a determinant of RGS2 function. J Biol Chem 274: 34253–34259.
- Kehrl JH, Sinnarajah S (2002) RGS2: a multifunctional regulator of G-protein signaling. Int J Biochem Cell Biol 34: 432–438.
- Salim S, Sinnarajah S, Kehrl JH, Dessauer CW (2003) Identification of RGS2 and type V adenylyl cyclase interaction sites. J Biol Chem 278: 15842–15849.
- Zhang S, Watson N, Zahner J, Rottman JN, Blumer KJ, et al. (1998) RGS3 and RGS4 are GTPase activating proteins in the heart. J Mol Cell Cardiol 30: 269–276.
- Erdely HA, Lahti RA, Lopez MB, Myers CS, Roberts RC, et al. (2004) Regional expression of RGS4 mRNA in human brain. Eur J Neurosci 19: 3125–3128.
- Watson N, Linder ME, Druey KM, Kehrl JH, Blumer KJ (1996) RGS family members: GTPase-activating proteins for heterotrimeric G-protein alpha-subunits. Nature 383: 172–175.
- Lan KL, Sarvazyan NA, Taussig R, Mackenzie RG, DiBello PR, et al. (1998) A point mutation in Galphao and Galphai1 blocks interaction with regulator of G protein signaling proteins. J Biol Chem 273: 12794–12797.
- Hollenberg MD, Compton SJ (2002) International Union of Pharmacology. XXVIII. Proteinase-activated receptors. Pharmacol Rev 54: 203–217.
- Vu TK, Hung DT, Wheaton VI, Coughlin SR (1991) Molecular cloning of a functional thrombin receptor reveals a novel proteolytic mechanism of receptor activation. Cell 64: 1057–1068.
- Coughlin SR (2005) Protease-activated receptors in hemostasis, thrombosis and vascular biology. J Thromb Haemost 3: 1800–1814.
- Traynelis SF, Trejo J (2007) Protease-activated receptor signaling: new roles and regulatory mechanisms. Curr Opin Hematol 14: 230–235.
- McCoy KL, Traynelis SF, Hepler JR (2010) PAR1 and PAR2 couple to overlapping and distinct sets of G proteins and linked signaling pathways to differentially regulate cell physiology. Mol Pharmacol 77: 1005–1015.
- McCoy KL, Gyoneva S, Vellano CP, Smrcka AV, Traynelis SF, et al. (2012) Protease-activated receptor 1 (PAR1) coupling to G (q/11) but not to G (i/o) or G (12/13) is mediated by discrete amino acids within the receptor second intracellular loop. Cell Signal 24: 1351–1360.
- Vellano CP, Maher EM, Hepler JR, Blumer JB (2011) G protein-coupled receptors and resistance to inhibitors of cholinesterase-8A (Ric-8A) both regulate the regulator of G protein signaling 14 RGS14.Galphai1 complex in live cells. J Biol Chem 286: 38659–38669.
- Vellano CP, Brown NE, Blumer JB, Hepler JR (2013) Assembly and function of the regulator of G protein signaling 14 (RGS14).H-Ras signaling complex in live cells are regulated by Galphai1 and Galphai1-linked G protein-coupled receptors. J Biol Chem 288: 3620–3631.
- Saugstad JA, Marino MJ, Folk JA, Hepler JR, Conn PJ (1998) RGS4 inhibits signaling by group I metabotropic glutamate receptors. J Neurosci 18: 905–913.
- Gutkind JS (1998) The pathways connecting G protein-coupled receptors to the nucleus through divergent mitogen-activated protein kinase cascades. J Biol Chem 273: 1839–1842.
- Buhl AM, Johnson NL, Dhanasekaran N, Johnson GL (1995) G alpha 12 and G alpha 13 stimulate Rho-dependent stress fiber formation and focal adhesion assembly. J Biol Chem 270: 24631–24634.

30. Gohla A, Harhammer R, Schultz G (1998) The G-protein G13 but not G12 mediates signaling from lysophosphatidic acid receptor via epidermal growth factor receptor to Rho. *J Biol Chem* 273: 4653–4659.
31. Zhong H, Neubig RR (2001) Regulator of G protein signaling proteins: novel multifunctional drug targets. *J Pharmacol Exp Ther* 297: 837–845.
32. Day PW, Wedegaertner PB, Benovic JL (2004) Analysis of G-protein-coupled receptor kinase RGS homology domains. *Methods Enzymol* 390: 295–310.
33. Gibson SK, Gilman AG (2006) Galpha and Gbeta subunits both define selectivity of G protein activation by alpha2-adrenergic receptors. *Proc Natl Acad Sci U S A* 103: 212–217.
34. Oner SS, Maher EM, Breton B, Bouvier M, Blumer JB (2010) Receptor-regulated interaction of activator of G-protein signaling-4 and Galphai. *J Biol Chem* 285: 20588–20594.
35. Bockaert J, Fagni L, Dumuis A, Marin P (2004) GPCR interacting proteins (GIP). *Pharmacol Ther* 103: 203–221.
36. Verrall S, Ishii M, Chen M, Wang L, Tram T, et al. (1997) The thrombin receptor second cytoplasmic loop confers coupling to Gq-like G proteins in chimeric receptors. Additional evidence for a common transmembrane signaling and G protein coupling mechanism in G protein-coupled receptors. *J Biol Chem* 272: 6898–6902.
37. Hepler JR (1999) Emerging roles for RGS proteins in cell signalling. *Trends Pharmacol Sci* 20: 376–382.
38. Ghil S, Choi JM, Kim SS, Lee YD, Liao Y, et al. (2006) Compartmentalization of protein kinase A signaling by the heterotrimeric G protein Go. *Proc Natl Acad Sci U S A* 103: 19158–19163.
39. Strittmatter SM, Fishman MC, Zhu XP (1994) Activated mutants of the alpha subunit of G (o) promote an increased number of neurites per cell. *J Neurosci* 14: 2327–2338.
40. Jordan JD, He JC, Eungdamrong NJ, Gomes I, Ali W, et al. (2005) Cannabinoid receptor-induced neurite outgrowth is mediated by Rap1 activation through G (alpha) o/i-triggered proteasomal degradation of Rap1GAPII. *J Biol Chem* 280: 11413–11421.
41. Chen B, Siderovski DP, Neubig RR, Lawson MA, Trejo J (2014) Regulation of protease-activated receptor 1 signaling by the adaptor protein complex 2 and R4 subfamily of regulator of G protein signaling proteins. *J Biol Chem* 289: 1580–1591.